Detailed Description of Simulation Steps

The simulation is performed for unique events *e*. Here, *e* corresponds to either the hypothesized Younger Dryas Impact or the Laacher See Volcanic Eruption. For each event *e*, we performed the simulation for 10,000 iterations in each year $x_{e,i}$ in a vector x_e of calendar years. For the former event, we used dates corresponding to the purported Younger Dryas Boundary (YDB), and for the latter event we used dates associated with the Laacher See Tephra (LST). For the YDB, x_{YDB} spans 151 years within 12,860—12,710 cal BP, and for the LST, x_{LST} spans 151 years within 12,991—12,841 cal BP. The central 101 years in each x_e corresponds to a range of possible calendar years for each hypothesized event. We simulated over a 25-year buffer on each side of the hypothesized range to observe how expectations vary for calendar years proximate to the possible calendar years for each hypothesized event.

For each of the 10,000 iterations in year $x_{e,i}$, the simulation performs four main steps:

(1) A vector of true calendar ages *C* is selected for the synchronous event. The length of *C* depends on the number of ^{14}C measurements in the observed sample (30 for the YDB and 19 for the LST).
(2) Expected target ^{14}C values are generated for each calendar age in *C*.
(3) For each target ^{14}C value, an expected ^{14}C value as *measured* by a laboratory is generated.
(4) Each measured ^{14}C value is calibrated with the IntCal13 ^{14}C calibration curve (1).

The remainder of this section describes each of the four steps. These descriptions concern a single iteration for a single calendar age $x_{e,i}$. To help illustrate these steps, Table S1.1 provides a toy set of reported ^{14}C measurements that could be used as simulation input for a hypothetical synchronous event. We expand on this table with each simulation step. All references to "calendar ages/years/dates" indicate years BP. AMS refers to accelerator mass spectrometry, GPC refers to gas proportional counting, and LSC refers to liquid scintillation counting.

1.1. True Calendar Ages

For each iteration within calendar year $x_{e,i}$, a vector of repeating $x_{e,i}$ values is first generated. The length of this vector is determined by the existing ^{14}C datasets for each event. The YDB dataset consists of 30 reported dates, which creates a vector of 30 $x_{e,i}$ values for these simulations. The corresponding LST vector length is 19. For simulations that lack "old wood" effects, these repeated vectors are treated as the true calendar ages for each simulated ^{14}C measurement.

Some versions of the simulation account for "old wood" effects with an "old wood" model (OWM). These versions add a calendar year offset to each $x_{e,i}$. Additional years are added only to the $x_{e,i}$ values that correspond to dated materials from organisms that may have died prior to the event of interest. 24 of 30 reported YDB dates originate from such materials, and 18 of 19 reported LST dates correspond to these materials. Short-lived samples, such as those from grasses or seeds, do not receive age offsets. The new vector of calendar years that includes offset values is referred to here as x_e^O (Table S1.2).

Table S1.1. A toy dataset of reported ^{14}C measurements for five samples associated with a hypothesized event e. These measurements were made by three laboratories with codes ABCD, EFGH, and IJKLM. The first and last laboratories measure ^{14}C via AMS, while EFGH measures ^{14}C via GPC. Three of the five measurements are on wood, indicating that they may correspond to calendar ages older than the event of interest. The simulation generates expected ^{14}C values

(i.e., what might be observed in the μ column given a true synchronous event), while all other columns in this table provide context dependent input for the simulation itself.

	Reported ^{14}C			
Sample ID	**μ**	**σ**	**"old wood"?**	**Lab type**
ABCD-0001	10,251	25	No (seed)	AMS
ABCD-0002	10,290	35	No (seed)	AMS
EFGH-0001	10,295	75	Yes (wood)	GPC
EFGH-0003	10,299	55	Yes (wood)	GPC
IJKLM-0001	10,321	40	Yes (wood)	AMS

OWM age offsets are drawn randomly from an exponential distribution, with offsets near zero more likely. In other words, OWM offsets assume that organism death most likely occurred shortly before the calendar year of the event *e*, with the probability of an earlier death event decreasing with temporal distance from event *e*. We considered two exponential distributions, one with the λ parameter set to 0.04 and one with λ set to 0.01 (Figure S1.1). The former distribution is a conservative scenario in which old samples predate the event by few years (μ = 25, 95% HDI = 0—75), while the latter distribution results in larger age offsets on average (μ = 100, 95% HDI = 0—300; Figure S1.1b,c). New values are drawn from each exponential distribution for each of the 10,000 iterations, allowing for λ specific variability in "old wood" effects to be estimated across 10,000 iterations. These distributions were selected to bound the extremes of realistic offsets that might be expected given "old wood" effects.

Table S1.2. The initial step in a single simulation iteration. Here, the toy dataset is used as input for a simulation iteration at 12,000 cal BP. The reported ^{14}C means have been removed, as these do not serve as input for the simulation. The age offsets are shown for hypothetical values drawn from an exponential distribution with λ = 0.04.

	Reported ^{14}C						
Sample ID	**μ**	**σ**	**"old wood"?**	**Lab type**	$x_{e,i}$	**Offset**	$x_{e,i}^{o}$
ABCD-0001	-	25	No	AMS	12,000	N/A	12,000.0
ABCD-0002	-	35	No	AMS	12,000	N/A	12,000.0
EFGH-0001	-	75	Yes	GPC	12,000	27.5	12,027.5
EFGH-0003	-	55	Yes	GPC	12,000	6.1	12,006.1
IJKLM-0001	-	40	Yes	AMS	12,000	88.5	12,088.5

Most of the wood samples for Laacher See are *Populus* (2), which is most likely Eurasian aspen (*Populus tremula*) or black poplar (*Populus nigra*). The former species lives an average of 50-100 years (3) and can live up to 200 years (4). In contrast, black popular generally live only 20-50 years. As such, the conservative exponential model (λ = 0.04) generally gives offsets intermediate between the lifespans of these species (Figure S1.1b). The latter "old wood" exponential function (λ = 0.01) is more consistent with aspen and produces occasional offsets several centuries older than the lifespan of aspen (Figure S1.1c). This can accommodate scenarios in which dead wood on the landscape is incorporated into the geological stratum of interest. We assume that true "old wood" effects for the YDB and LST wood and charcoal ^{14}C samples fall somewhere between the two extremes defined by these exponential functions, and neither exponential function is intended to match precisely the "old wood" effects in either context, which are probably unknowable.

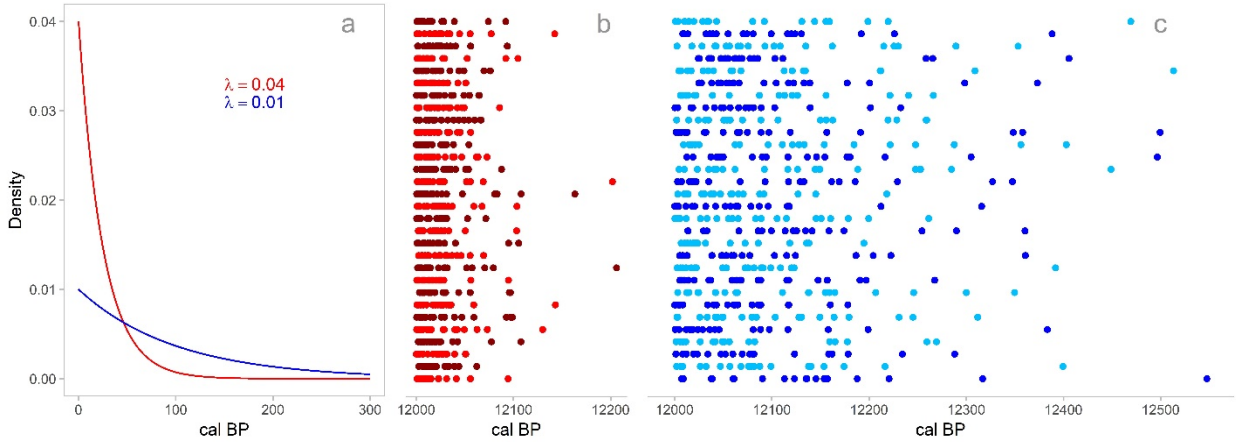

Figure S1.1. Exponential distributions used for versions of the simulation employing an OWM. (a) Probability density functions for each offset. (b and c) 30 examples of 20 "old wood" dates for a synchronous event at 12,000 cal BP, where each row is a sample of 20 dates. Panel b corresponds to an exponential distribution with λ = 0.04, and panel c corresponds to an exponential distribution with λ = 0.01.

1.2. Target ^{14}C Values

We generated a target ^{14}C value for each $x_{e,i}^{O}$ value in two steps. First, mean ^{14}C values were obtained by "uncalibrating" $x_{e,i}^{O}$ values with the *uncalibrate* function in the *rcarbon* R package (5)**.** This function works by drawing from a normal distribution of ^{14}C values associated with a calendar year, where the distribution corresponds to the calibration curve error in the IntCal13 ^{14}C calibration curve (Figure S1.2a). This produces a hypothetical mean atmospheric ^{14}C value for the calendar year (Table S1.3). $x_{e,i}^{O}$ that share identical values receive the same uncalibrated mean atmospheric ^{14}C value since they correspond to a calendar year with the sample hypothetical mean atmospheric ^{14}C value. Mean atmospheric ^{14}C values are resampled for each of the 10,000 iterations.

Second, we account for intra-annual variability around the mean atmospheric ^{14}C value in a calendar year. We estimated the difference between seasonal extremes of atmospheric ^{14}C variability using data from McDonald et al. (6). They estimate the distance between seasonal extremes of atmospheric ^{14}C with two calculation methods, each of which is performed for situations in which atmospheric ^{14}C production is in increasing and decreasing states (Table S1.4). We also consider stable atmospheric ^{14}C production, treated here as the midpoint between McDonald et al.'s (6) values for increasing and decreasing production.

Table S1.3. The first part of step two for a single simulation iteration. Here, the toy dataset is used as input for a simulation iteration at 12,000 cal BP. The reported ^{14}C means have been removed, as these do not serve as simulation input. Mean atmospheric ^{14}C values have been sampled from the IntCal13 ^{14}C calibration curve error distribution around each calendar age $x_{e,i}^{O}$.

	Reported ^{14}C					
Sample ID	**μ**	**σ**	**"old wood"?**	**Lab type**	**$x_{e,i}^{O}$**	**Mean atmospheric ^{14}C**

ABCD-0001	-	25	No	AMS	12,000.0	10,222
ABCD-0002	-	35	No	AMS	12,000.0	10,222
EFGH-0001	-	75	Yes	GPC	12,027.5	10,261
EFGH-0003	-	55	Yes	GPC	12,006.1	10,300
IJKLM-0001	-	40	Yes	AMS	12,088.5	10,366

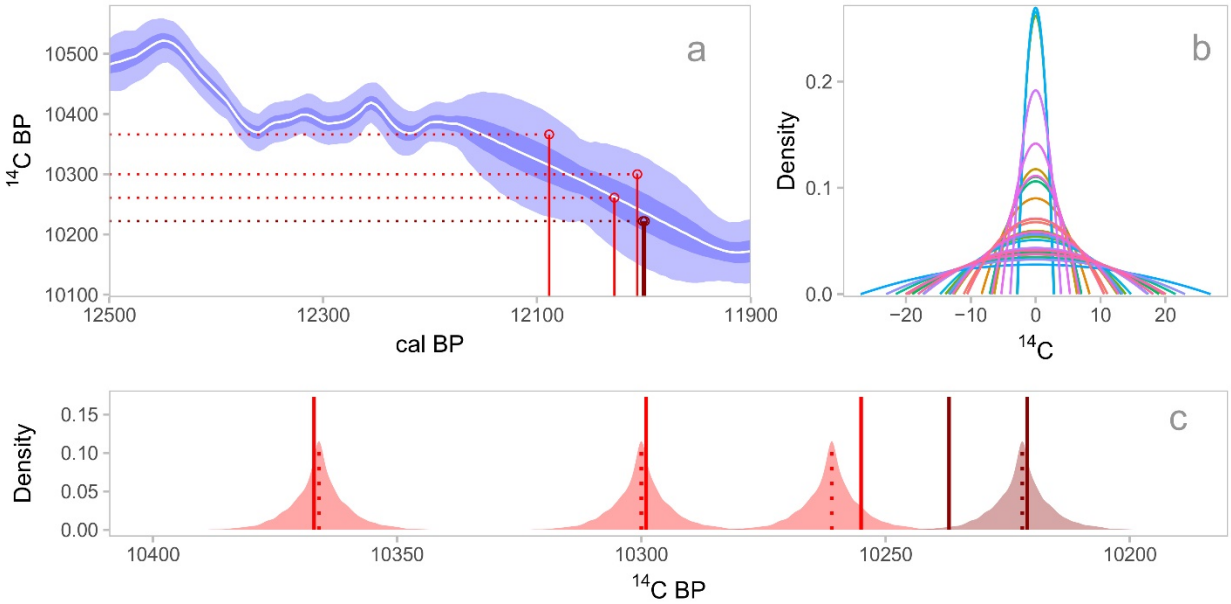

Figure S1.2. A visual schematic of simulated target ^{14}C values based on context dependent input from the toy dataset: (a) "Uncalibrating" five calendar ages (i.e., converting $x_{e,i}^{O}$ values into mean atmospheric ^{14}C values; Table S1.3 for details). The blue calibration curve bands show the 50% and 95% error regions, and the white line shows the mean value of the curve. (b) 30 randomly sampled beta distributions that represent possible intra-annual distributions of ^{14}C variability. (c) Mean "uncalibrated" ^{14}C values (dotted lines), intra-annual ^{14}C variability around those values based on 10,000 randomly sampled beta distributions (red semitransparent regions), and ^{14}C values sampled from those intra-annual ^{14}C variability distributions (solid lines). The ^{14}C values sampled from each intra-annual distribution comprise the target ^{14}C values. These are the values that laboratories attempt to measure. In panels a and c, light red geometry corresponds to three calendar ages with "old wood" effects, and dark red geometry corresponds to two overlapping calendar ages that date the event of interest.

Table S1.4. Estimates of the intra-annual distance between atmospheric ^{14}C extremes ((6) for increasing and decreasing values. The stable values are the midpoints between the increasing and decreasing values).

Intra-annual distance	Error	Atmospheric ^{14}C trend	Calculation method
18.0	13.0	Increasing	First
23.0	16.0	Decreasing	First
20.5	14.5	Stable	First

26.0	16.0	Increasing	Second
22.0	13.0	Decreasing	Second
24.0	14.5	Stable	Second

To estimate intra-annual atmospheric ^{14}C variability, we first modelled possible values as sparsely beta distributed *β(2, 2)*, centered on 0, and scaled by the intra-annual distance. Since the intra-annual distance is imprecisely known, we simulated 10,000 beta distributions scaled by samples drawn from *N(Intra-annual distance, Error)* (Figure S1.2b). For each of the 10,000 samples, we randomly selected one of the six possible distance and error pairings. Therefore, these distributions average across atmospheric ^{14}C production trends and calculation methods. For each of the 10,000 simulation iterations, a random value is drawn from one of the 10,000 centered and scaled beta distributions. This random value is then added to the mean atmospheric ^{14}C value to estimate a target ^{14}C value that reflects both inter- and intra-annual ^{14}C variability (Table S1.5; Figure S1.2c).

Table S1.5. The second part of step two for a single simulation iteration. Here, the toy dataset is used as input for a simulation iteration at 12,000 cal BP. The reported ^{14}C means have been removed, as these do not serve as input for the simulation.

Sample ID	Reported ^{14}C		"old wood"?	Lab type	Mean atmospheric ^{14}C	Intra-annual variation offset	Target ^{14}C
	μ	σ					
ABCD-0001	-	25	No	AMS	10,222	15	10,237
ABCD-0002	-	35	No	AMS	10,222	-1	10,221
EFGH-0001	-	75	Yes	GPC	10,261	-6	10,255
EFGH-0003	-	55	Yes	GPC	10,300	-1	10,299
IJKLM-0001	-	40	Yes	AMS	10,366	1	10,367

1.3. Measured ^{14}C Values

Given minor inter-laboratory variability that conditions systematic biases, as well as minor instrumental error that shapes intra-laboratory measurement repeatability, measured ^{14}C values depart from their target values (7–12). As such, the dispersion of reported ^{14}C values should vary based on the number of laboratories that have contributed to a reported ^{14}C dataset, as well as based on laboratory specific characteristics that might further influence the repeatability of measurements. These sources of inter- and intra-laboratory variability can be used to model expected departures of ^{14}C measurements from their target values, given known numbers of laboratories and measurements per laboratory.

To estimate this variability, we fit a Bayesian multilevel model to data reported in the Fifth International Radiocarbon Intercomparison (VIRI) (7, 13, 14). We refer to this model as the Laboratory Measurement Bias and Repeatability Model, or LBM. The LBM treats ^{14}C measurements as a normally distributed outcome. We defined a three-parameter linear model for the outcome mean: a categorical intercept for each sample material, a random categorical effect for laboratory ID, and a scaling parameter that adjusts the random laboratory ID effect based on whether the laboratory performs AMS or GPC/LSC measurements. We defined a four-parameter linear model for the outcome standard deviation. Parameters consist of a baseline intercept, a random categorical effect for laboratory ID, a linear effect for reported measurement error, and a categorical effect that accounts for whether laboratories perform AMS or GPC/LSC

measurements. Section 3 describes this model in detail, including the model formula, prior distributions for model parameters, and a posterior predictive check.

The simulation samples 10,000 sets of values from the posterior distributions of the LBM parameters, with a unique set of parameter values applied to each of the 10,000 simulation iterations (Figure S1.3). Therefore, uncertainty in the model parameters is distributed across iterations within each calendar year $x_{e,i}$:

1. A random offset from the target ^{14}C value representing the mean observed value within each laboratory. The number of sampled offsets is determined by the number of laboratories that contributed to the reported ^{14}C dataset (Table S1.6).
2. A multiplier term that rescales the offset for GPC/LSC laboratories (Table S1.6).
3. A random within-laboratory standard deviation that is rescaled by an additional multiplier value for GPC/LSC laboratories (σ_L). This standard deviation further varies by the error reported for each ^{14}C measurement (Table S1.7).
4. Values are then drawn from laboratory and sample specific distributions defined by *N(Mean laboratory specific ^{14}C, σ_L)*, representing ^{14}C values that might be measured by each laboratory (Table S1.8).

The standard deviation for expected within lab measured ^{14}C variability depends on the reported error of the sample (σ). It takes the form,

$$\sigma_L = \exp(Lab\ effect + GPC|LSC\ effect + \log(\sigma) * \sigma\ effect) * 100.01. \quad \text{(Equation S1.1)}$$

Possible values for each effect are presented in Table S1.7. The 100.01 value to the right of the exponential transformation puts the result on the scale of ^{14}C years (the LBM is fitted to ^{14}C year z-scores, and therefore, the output of this linear model needs to be put back on the ^{14}C year scale).

The measured ^{14}C values comprise an expected set of observations generated for a single iteration. The simulation records the expected standard deviation of these values, $^{14}C_E^{\sigma}$ (69.8 for the toy dataset detailed here), as a measure of dispersion for a series of ^{14}C measurements, given a synchronous event. This is completed over 10,000 iterations for each calendar year $x_{e,i}$, yielding a distribution of $^{14}C_E^{\sigma}$ given the number of labs, lab types (AMS or GPC/LSC), reported measurement errors, and potential "old wood" effects associated with a reported ^{14}C dataset. For versions of the simulation that exclude the LBM, these $^{14}C_E^{\sigma}$ values are calculated with the target ^{14}C values rather than the measured ^{14}C values (as calculated in Step 2).

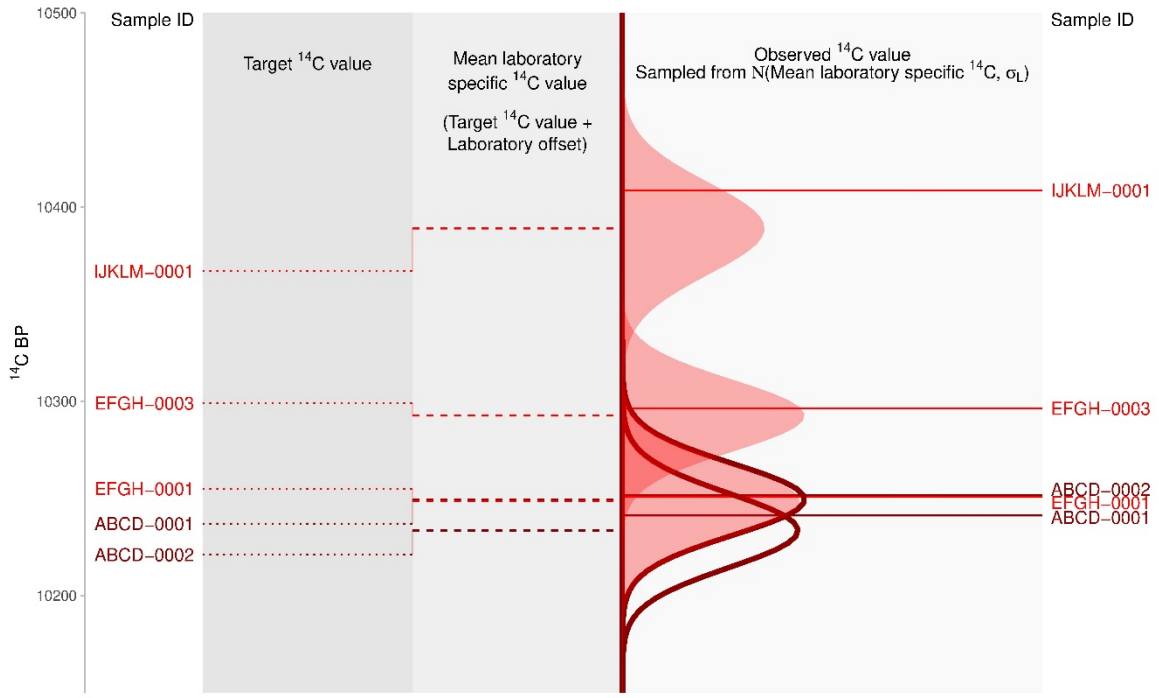

Figure S1.3. An example of five target ^{14}C values being converted to measured ^{14}C values via sampling from the LBM. Refer to Tables S1.6, S1.7, and S1.8 for the values depicted in this figure. Light red lines correspond to three calendar ages with "old wood" effects, and dark red lines correspond to two calendar ages that date the event of interest. Rotated normal distributions illustrate intra-laboratory sampling distributions for each measured ^{14}C value; They correspond to the distribution of repeated measurements for a given laboratory at a given reported measurement error, centered on the mean laboratory specific ^{14}C value for a target ^{14}C value. Two normal distributions with empty fills and dark red outlines depict calendar ages that lack "old wood" effects, and three normal distributions with light red fills and no outlines show calendar ages with "old wood" effects. Note, the intra-laboratory sampling distributions for ABCD-0001 and EFGH-0001 overlap nearly completely, and the values sampled for ABCD-002 and EFGH-0001 are very similar.

Table S1.6. Obtaining mean laboratory offset values for measured ^{14}C in a single simulation iteration. Here, the toy dataset is used as input for a simulation iteration at 12,000 cal BP. The reported ^{14}C means have been removed, as these do not serve as input for the simulation. The laboratory offset and GPC/LSC multiplier values are sampled from the LBM parameters, which vary across the 10,000 simulation iterations.

	Reported ^{14}C			Target	Lab	GPC|LSC	Mean lab
Sample ID	**μ**	**σ**	**Lab type**	**^{14}C**	**offset**	**multiplier**	**specific ^{14}C**
ABCD-0001	-	25	AMS	10,237	12.5	N/A	10,249.5
ABCD-0002	-	35	AMS	10,221	12.5	N/A	10,233.5
EFGH-0001	-	75	GPC	10,255	-5.8	1.1	10,248.6
EFGH-0003	-	55	GPC	10,299	-5.8	1.1	10,292.6
IJKLM-0001	-	40	AMS	10,367	22.0	N/A	10,389.0

Table S1.7. Parameters for sampling measured ^{14}C values. Here, the toy dataset is used as input for a simulation iteration at 12,000 cal BP. The reported ^{14}C means have been removed, as these do not serve as input for the simulation. Laboratory effects, GPC/LSC effects, and σ effects are sampled from the posterior distributions of the LBM parameters, which vary across the 10,000 simulation iterations.

	Reported ^{14}C		Lab	Mean lab	Within lab std. deviation (σ_L) parameters		
Sample ID	**μ**	**σ**	**type**	**specific ^{14}C**	**Lab effect**	**GPC|LSC effect**	**σ effect**
ABCD-0001	-	25	AMS	10,249.5	-2.1	N/A	0.35
ABCD-0002	-	35	AMS	10,233.5	-2.1	N/A	0.35
EFGH-0001	-	75	GPC	10,248.6	-2.5	0.32	0.35
EFGH-0003	-	55	GPC	10,292.6	-2.5	0.32	0.35
IJKLM-0001	-	40	AMS	10,389.0	-1.9	N/A	0.35

Table S1.8. Sampled measured ^{14}C values. Here, the toy dataset is used as input for a simulation iteration at 12,000 cal BP. The reported means have been removed, as these do not serve as input for the simulation. Lab/sample deviations were calculated with the "Within lab std. deviation parameters" from Table S1.7 using Equation S1.1.

	Reported ^{14}C		Lab	Within lab sampling parameters		
Sample ID	**μ**	**σ**	**type**	**^{14}C μ**	**Std. deviation (σ_L)**	**Measured ^{14}C value**
ABCD-0001	-	25	AMS	10,249.5	18.4	10,241.2
ABCD-0002	-	35	AMS	10,233.5	19.1	10,251.7
EFGH-0001	-	75	GPC	10,248.6	18.9	10,250.8
EFGH-0003	-	55	GPC	10,292.6	18.4	10,296.3
IJKLM-0001	-	40	AMS	10,389.0	23.6	10,408.6

1.4. Calibrated ^{14}C Measurements

The simulation then calibrates the measured ^{14}C values using the errors described in the reported dataset, producing a probability density across calendar ages for each measurement (Table S1.9; Figure S1.4). This is accomplished with the IntCal13 curve using the *calibrate* function in the *rcarbon* R package (5).

Table S1.9. Sampled measured ^{14}C values and the 95% highest density intervals (HDI) for their calibrated age densities. Here, the toy dataset is used as input for a simulation iteration at 12,000 cal BP. The reported means have been removed, as these do not serve as input for the simulation. Note that the measured ^{14}C values in the simulation are calibrated with σ values for the reported measurements.

	Reported ^{14}C		Measured ^{14}C		
Sample ID	**μ**	**σ**	**μ**	**σ**	**Cal BP (95% HDIs)**
ABCD-0001	-	25	10,241.2	25	12,111—11,921; 11,915—11,827
ABCD-0002	-	35	10,251.7	35	12,130—11,826
EFGH-0001	-	75	10,250.8	75	12,384—12,264; 12,246—11,711
EFGH-0003	-	55	10,296.3	55	12,386—12,262; 12,249—11,929; 11,894—11,829
IJKLM-0001	-	40	10,408.6	40	12,517—12,482; 12,424—12,085

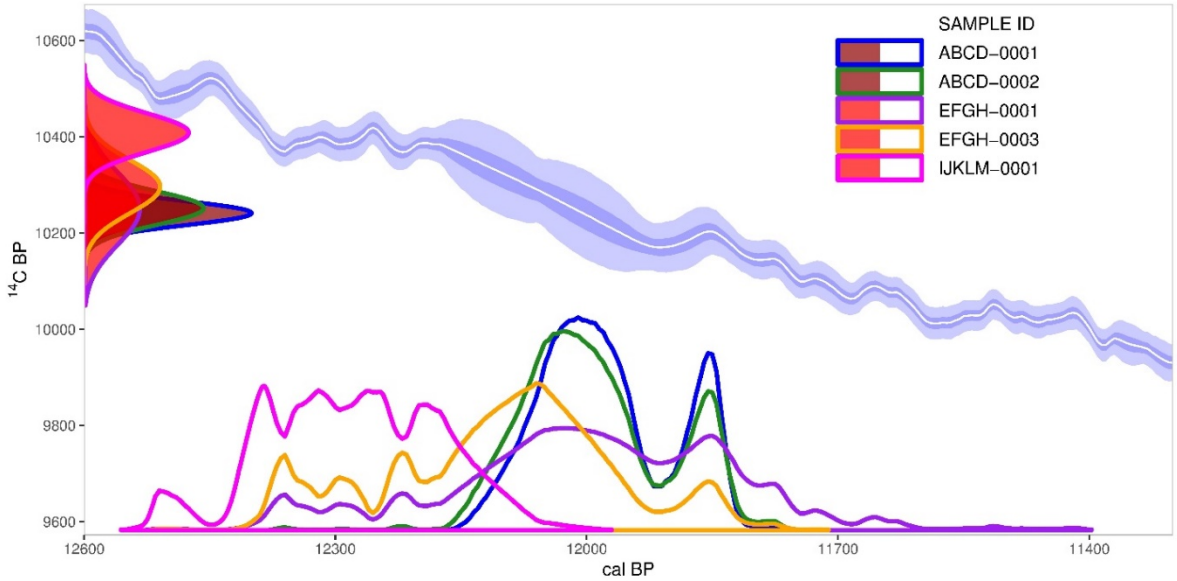

Figure S1.4. Toy dataset: Five expected ^{14}C measurements (rotated normal distributions) calibrated with the IntCal13 calibration curve (white line with blue bands). The blue calibration curve bands show the 50% and 95% error regions and the white line depicts the mean curve value. Light red geometry corresponds to three samples with "old wood" effects, and dark red geometry corresponds to two overlapping samples that date the event of interest. The undulating distributions on the x-axis depict calibrated age densities, which are used to calculate the MPMD.

Following calibration, Manhattan distances are then calculated for each pair of age densities (Table S1.10):

$$Manhattan\ distance = \sum_{i=1}^{c} \left| A_{x,i} - A_{y,i} \right|,$$

(Equation S1.2)

where $A_{x,i}$ indexes a density value for calendar year i in age density A_x, $A_{y,i}$ indexes a density value in age density A_y for calendar year i, and c is the length of a vector that comprises the union of calendar ages shared by the pair of age densities. The expected Mean Pairwise Manhattan Distance ($MPMD_E$) is then calculated by taking the mean of all pairwise distances and dividing this mean by two. A value of exactly zero indicates that the age densities are identical, while a value of exactly one indicates that the set of age densities are completely nonoverlapping. Like the $\sigma_{\mu^{14}C}$ values calculated at the end of Step 3, 10,000 $MPMD_E$ values are obtained for each year $x_{e,I}$ across the iterations.

Table S1.10. Manhattan distances between each pair of the five calibrated age distributions in the toy dataset. The mean of these values is divided by two to obtain the $MPMD_E$ (0.508 for this toy dataset). Here, the toy dataset is used as input for a simulation iteration at 12,000 cal BP.

	ABCD-001	ABCD-002	EFGH-001	EFGH-003	IJKLM-001
ABCD-001					
ABCD-002	0.187				
EFGH-001	0.705	0.618			
EFGH-003	0.946	0.799	0.631		
IJKLM-001	1.860	1.805	1.478	1.136	

Citations

1. Reimer PJ, et al. (2013) IntCal13 and Marine13 radiocarbon age calibration curves 0–50,000 years cal BP. *Radiocarbon* 55(4):1869–1887.

2. Baales M, et al. (2002) Impact of the Late Glacial Eruption of the Laacher See Volcano, Central Rhineland, Germany. *Quat Res* 58(03):273–288.

3. Caudullo G, de Rigo D (2016) Populus tremula in Europe: distribution, habitat, usage and threats. *European Atlas of Forest Tree Species.*, eds San-Miguel-Ayanz J, de Rigo D, Caudullo G, Houston T, Mauri A (Publication Office of the European Union, Luxembourg), pp 138–139.

4. von Wühlisch G (2009) *EUFORGEN Technical Guidelines for genetic conservation and use for Eurasian aspen (Populus tremula)* (Biodiversity International, Rome).

5. Bevan A, Crema ER (2018) *rcarbon v1.2.0: Methods for calibrating and analyzing radiocarbon dates* Available at: https://CRAN.R-project.org/package=rcarbon.

6. McDonald L, Chivall D, Miles D, Bronk Ramsey C (2018) Seasonal variations in the 14C content of tree rings: influences on radiocarbon calibration and single-year curve construction. *Radiocarbon*:1–10.

7. Scott EM, Cook GT, Naysmith P (2010) The Fifth International Radiocarbon Intercomparison (VIRI): An Assessment of Laboratory Performance in Stage 3. *Radiocarbon* 52(03):859–865.

8. Boaretto E, et al. (2003) How reliable are radiocarbon laboratories? A report on the Fourth International Radiocarbon Inter-comparison (FIRI)(1998–2001). *Antiquity* 77(295):146–154.

9. Scott EM, Aitchison TC, Harkness DD, Cook GT, Baxter MS (1990) An Overview of All Three Stages of the International Radiocarbon Intercomparison. *Radiocarbon* 32(03):309–319.

10. Scott EM, Harkness DD, Cook Gt (1998) Interlaboratory comparisons: lessons learned. *Radiocarbon* 40(1):331–340.

11. International Study Group, et al. (1982) An inter-laboratory comparison of radiocarbon measurements in tree rings. *Nature* 298:619–623.

12. Scott EM, Cook GT, Naysmith P (2007) Error and Uncertainty in Radiocarbon Measurements. *Radiocarbon* 49(02):427–440.

13. Scott EM, Cook GT, Naysmith P, Bryant C, O'Donnell D (2007) A Report on Phase 1 of the 5th International Radiocarbon Intercomparison (VIRI). *Radiocarbon* 49(02):409–426.

14. Scott EM, Cook GT, Naysmith P (2010) A Report on Phase 2 of the Fifth International Radiocarbon Intercomparison (VIRI). *Radiocarbon* 52(03):846–858.